Indian Journal of Chemistry
Vol. 60B, December 2021, pp. 1652-1658

Crystal structure determination, molecular modeling and surface analysis studies of 2-(4,6-dihydropyren-3-yl)-1*H*-benzodimidazole

R Manickam[a], R Jagan[b], G Jagadeesan[c] & G Srinivasan*[a]

[a] PG and Research Department of Physics, Government Arts College for Men (Autonomous), University of Madras, Nandanam, Chennai 600 035, India

[b] Sophisticated Analytical Instrument Facility (SAIF), Indian Institute of Technology Madras, Chennai 600 036, India

[c] Department of Physics, Jeppiaar Engineering College, Jeppiaar Nagar, OMR, Chennai 600 119, India

E-mail: agsv71@gmail.com

Received 31 May 2020; accepted (revised) 23 August 2021

Benzoimidazole compound has been synthesized and structurally characterized by single crystal X-ray diffraction studies, molecular docking and Hirshfeld surface analysis. The title compound C23 H14 N2 crystallizes in the Orthorhombic crystal system with the crystallographic space group of $Pna2_1$ with cell parameters a = 9.4472(5)Å, b=9.0556(5)Å, c=18.3755(11)Å, V=1572.03(15)Å^3 and Z=4. The structure exhibits various intra and intermolecular interactions of the type N-H...N. Molecular docking studies of benzoimidazole compound have been executed with Cancer Osaka Thyroid kinease target protein which shows high binding affinity. In addition to this, Hirshfeld surface computational analysis have been carried out to analysis the hydrogen bond interaction. The major intermolecular contacts contributing to the Hirshfeld surface are H...H, H...N and H...C, respectively.

Keywords: Benzoimidazoles, crystal structure, anticancer, Hirshfeld Surfaces

Benzoimidazoles moieties are an vital role of heterocyclic compounds contain nitrogen having great importance in the field of pharmaceutical industry, among heterocycles benzoimidazole occupied most significant place due to its diverse biological activities and the studies due to their broad range of applications (Gharib *et al*., 2014) such as angiotensin inhibitors (Trujillo *et al*., 2009), glucagon antagonist (Chang *et al*., 2001) and high cytotoxicity, which has preferable them as new drug in cancer therapy (King *et al*., 2006). The compound is a unique heterocyclic structure containing a benzene ring fused to an imidazole ring. The influence of the imidazoles can be attributed to its hydrogen bond donor-acceptor capability in addition to its high affinity for metals (e.g., Zn, Fe, Mg), which are found in many protein active sites.

The benzophenone is an important organic compound used as a building block of many pharmaceutical compounds on its numerous biological activities such as anti-inflammatory, anticancer and so many activity (Winter et al., 1962), hence in the benzophenone compound is fused to benzoimidazoles to enhance more biological activities, subsequently we performed molecular docking for anti-cancer target with kinase protein is Cancer Osaka Thyroid Kinase protein and reported as better binding energy than previously reported ones, hence we report structural, molecular docking and Hirshfeld surfaces analysis studies of 2-(4,6-dihydropyren-3-yl)-1H-benzodimidazole (Figure 1).

Materials and Methods

Synthesis of 2-(4,6-dihydropyren-3-yl)-1*H*-benzodimidazole

Suitable proportions of o-phenylenediamine (1.08g; 10mmol) and 1-pyrenecarboxaldehyde (2.30g; 10mmol) were mixed in 30 ml of acetonitrile thoroughly, followed by heating and stirring for about one hour. Resultant solution was cooled to room temperature forming a precipitate. The precipitate was collected by filtration, dried and ground using agate mortar in the presence of acetone (Scheme I). Finely powdered title compound was dissolved in mixed

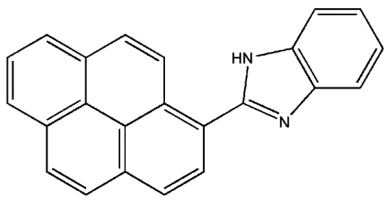

Figure 1 — Schematic diagram of benzodimidazole compound

solvents of ethanol and chloroform and kept for crystallization by slow evaporation method.

X-ray crystallography

Single crystal x-ray diffraction intensity data have been collected for benzoimidazole compound on Bruker axs Kappa ApexII (Bruker, 2008) equipped with graphite mono-chromated MoKα (λ=0.7103 Å) radiation and CCD detector. The unit cell parameters have been determined from 36 frames measured (0.5° phiscan) from three different crystallographic zones and using the method of difference vectors. The intensity data collection, frames integrations (Lorentz and polarization) and decay correction have been done using SAINT-NT (version 7.06) (Bruker, 2008) software. Empirical absorption correction (multi-scan) has been performed using SADABS (Bruker, 2008) program. Crystal structures have been solved by direct methods using SHELXS-97 (Sheldrick, 2008). The phase sets with the best combined figure of merits reveal the positions of all non-hydrogen atoms in both the structures. The structures have been then refined by full-matrix least-squares procedures using SHELXL-97 (Sheldrick, 2008).

Results and Discussion

Crystallographic Studies

Crystals of benzoimidazole suitable for single crystal X-ray analysis were grown via slow evaporation mixed solvents of ethanol and chloroform solution at room temperature. ORTEP plot of the diagram along with the atom-labelling scheme is given in Figure 2. X-ray crystallographic analysis revealed that benzoimidazole crystallizes in the monoclinic space group Pna21 and Z=4, full crystallographic data are presented in Table I. Selected bond lengths and bond angles of the benzoimidazole are given in Table II, Table III and Table IV, respectively.

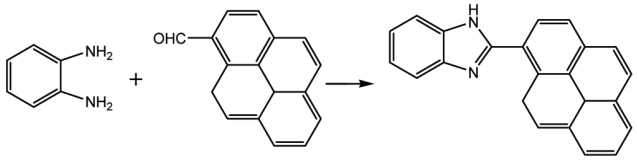

Scheme I

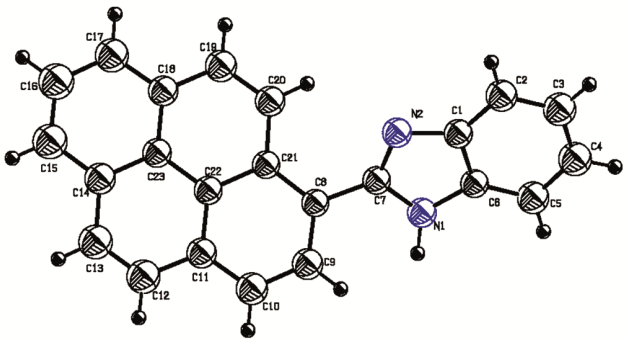

Figure 2 — ORTEP plot of the titled compound drawn at 50% of probability level

In benzimidazole moiety, C1-N2 bond of 1.390(5)° is formally treated as a double bond but N1-C6 = 1.379(5) is shortened comparing to the single C-N (1.47Å) bond. The C1-N2 bond is longer than C6-N1. This shortening of distance is due to electron delocalization in the ring.

The benzoimidazole ring [C1-C7/N1/N2] and pyrene ring [C8-C23] are planar conformation with maximum deviation of [C6=0.034(6) Å and C10=-0.052(7)Å], respectively. The dihedral angle between the benzoimidazole ring and pyrene ring makes an angle of 40.44(17)° bridged by the bond C7-C8. The values of torsion angles N2-C7-C8-C9= 34.7(5)° and N1-C7-C8-C21=39.5(6)°, benzophenones and pyrene

Table I — Crystal data and structure refinement details

Parameter	K21A
Empirical formula	C23 H14 N2
Formula weight	318.36
Temperature	293(2) K
Wavelength	0.71073 Å
Crystal system, space group	Orthorhombic, P n a 21
Unit cell dimensions	a = 9.4472(5) Å
	b = 9.0556(5) Å
	c = 18.3755(11) Å
Volume	1572.03(15) $Å^3$
Z, Calculated density	4, 1.345 Mg/m^3
Absorption coefficient	0.079 mm^{-1}
F(000)	664
Crystal size	0.300 x 0.250 × 0.200 mm
Theta range for data collection	2.217 to 24.987 º
Limiting indices	−10<=h<=11,
	−10<=k<=10,
	−21<=l<=21
Reflections collected / unique	21841 / 2768 [R_{int} = 0.0502]
Completeness to theta = 24.987	100.00%
Refinement method	Full-matrix least-squares on F^2
Data / restraints / parameters	2768 / 1 / 231
Goodness-of-fit on F^2	1.07
Final R indices [I>2sigma(I)]	R1 = 0.0370, wR2 = 0.0867
R indices (all data)	R1 = 0.0734, wR2 = 0.1119
Absolute structure parameter	−0.7(10)
Extinction coefficient	0.007(2)
Largest diff. peak and hole	0.150 and −0.152 e. $Å^{-3}$

Table II — Selected bond lengths (Å) and bond angles (°)

Bond	Length	Bond	Angle
C1-C2	1.389(5)	C2-C1-N2	130.4(3)
C1-N2	1.390(5)	C2-C1-C6	119.9(3)
C1-C6	1.390(5)	N2-C1-C6	109.7(3)
C2-C3	1.363(5)	C3-C2-C1	117.5(4)
C3-C4	1.375(6)	C2-C3-C4	122.2(4)
C4-C5	1.379(6)	C3-C4-C5	121.7(4)
C5-C6	1.384(5)	C4-C5-C6	116.1(4)
C6-N1	1.379(5)	N1-C6-C5	132.3(3)
C7-N2	1.316(5)	N1-C6-C1	105.0(3)
C7-N1	1.356(4)	C5-C6-C1	122.6(4)
C7-C8	1.474(5)	N2-C7-N1	112.1(3)
C8-C9	1.388(5)	N2-C7-C8	126.1(3)
C8-C21	1.400(5)	N1-C7-C8	121.4(3)
C9-C10	1.374(6)	C9-C8-C21	119.8(4)
C10-C11	1.386(6)	C9-C8-C7	117.1(3)
C11-C22	1.419(5)	C21-C8-C7	123.0(3)
C11-C12	1.431(6)	C10-C9-C8	121.3(4)
C12-C13	1.332(6)	C18-C23-C22	120.2(3)
C21-C22	1.426(5)	C14-C23-C22	120.0(4)
C22-C23	1.422(5)	C7-N1-C6	107.8(3)
N1-H1	0.90(4)	C7-N2-C1	105.4(3)

Table III — Selected torsion bond angles (°)

Torsion	Angle	Torsion	Angle
N2-C1-C2-C3	177.1(4)	C7-C8-C21-C20	6.6(5)
C6-C1-C2-C3	−0.8(6)	C19-C20-C21-C8	−179.5(4)
C1-C2-C3-C4	0.3(7)	C19-C20-C21-C22	1.1(5)
C2-C3-C4-C5	0.1(7)	C10-C11-C22-C23	177.8(3)
C3-C4-C5-C6	−0.1(6)	C12-C11-C22-C23	−2.1(5)
C4-C5-C6-N1	−176.2(4)	C10-C11-C22-C21	−2.9(5)
C4-C5-C6-C1	−0.4(6)	C12-C11-C22-C21	177.1(3)
C2-C1-C6-N1	177.7(4)	C8-C21-C22-C11	0.1(5)
N2-C1-C6-N1	−0.7(4)	C20-C21-C22-C11	179.6(3)
C2-C1-C6-C5	0.9(6)	C8-C21-C22-C23	179.3(3)
N2-C1-C6-C5	−177.4(4)	C20-C21-C22-C23	−1.2(5)
N2-C7-C8-C9	−137.0(4)	C17-C18-C23-C14	−0.4(5)
N1-C7-C8-C9	34.7(5)	C19-C18-C23-C14	179.7(3)
N2-C7-C8-C21	39.5(6)	C17-C18-C23-C22	179.9(3)
N1-C7-C8-C21	−148.8(3)	C19-C18-C23-C22	−0.1(5)
C12-C13-C14-C15	178.5(4)	N2-C7-N1-C6	−0.5(4)
C12-C13-C14-C23	−2.6(6)	C8-C7-N1-C6	−173.3(3)
C23-C14-C15-C16	−1.0(6)	C5-C6-N1-C7	177.0(4)
C13-C14-C15-C16	177.9(4)	C1-C6-N1-C7	0.7(4)
C14-C15-C16-C17	−0.2(7)	N1-C7-N2-C1	0.1(4)
C15-C16-C17-C18	1.1(7)	C8-C7-N2-C1	172.5(4)
C16-C17-C18-C23	−0.8(6)	C2-C1-N2-C7	−177.8(4)
C16-C17-C18-C19	179.1(4)	C6-C1-N2-C7	0.4(4)

Table IV — Geometric parameters of the intermolecular interactions (Å,°)

D-H...A	d(D-H)	d(H...A)	d(D...A)	<(DHA)
N1-H1...N2#1	0.90(4)	1.91(4)	2.796(4)	168(4)

Symmetry transformations used to generate equivalent atoms:
#1 x-1/2,-y+3/2,z

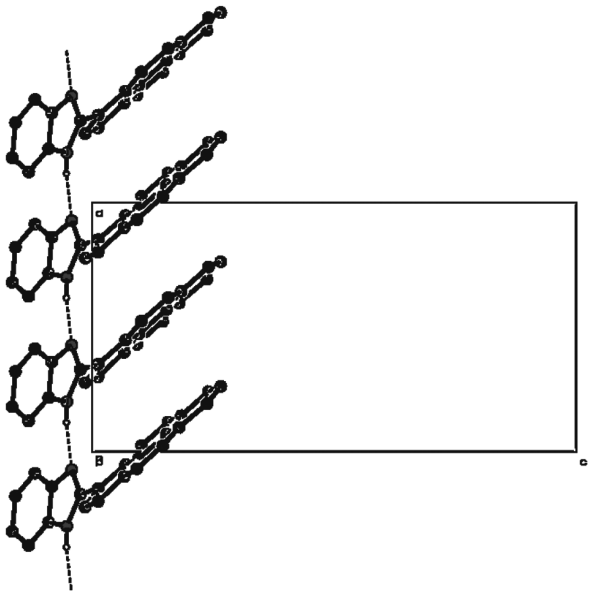

Figure 3 — Packing of the molecules when viewed along ‘c’ axis

torsion angles take the same sign and are each reported to be 30°.

Packing Features

The crystal packing arrangement shows the formation of (C4) chain running along ab plane (Figure 2). N-H…N hydrogen-bonds are observed between the adjacent molecules to form hydrogen bond (Table IV, Figure 3). Another non-prominent intramolecular C-H…N hydrogen bond and vander waals force are also present.

These hydrogen bonds add to the potential stability of the molecules within the crystal pack range (Figure 3), of the three-dimensional network structure. The crystal structure of benzoimidazole compound was studied using hirshfeld surface analysis study and confirmed using XRD analysis.

Molecular Docking

Protein preparation of COT kinase

Protein kinases play a very vital role in the cell biology where it can modify the functioning of a protein in the cell. Protein phosphorylation is a process which can increase or decrease the enzyme activity to alter the

cellular processes like transcription and translation and play a major role in signal transduction pathways which can activate other protein to be functioned. [Roskoski, 2015; London, 2013].

One of the protein kinase is Cancer Osaka Thyroid Kinase which is a Mitogen Activated Protein Kinase 8 (MAP3K8) (Figure 4). It involve to regulate various signaling pathways like cell survival, cell proliferation and cell death as well as various inflammatory pathways including ERK, JNK, p38, NFκB and plays an important role in the immune system also.

Computational Methods

The study reveals to demonstrate benzodimidazole derivative bind to Cancer Osaka Thyroid Kinase enzyme and to evaluate whether these molecules can be used as potential drug. The crystal structural information and target molecules were collected from the "Protein Data Bank" (PDB: 4Y83) (Gutmann et al., 2015).

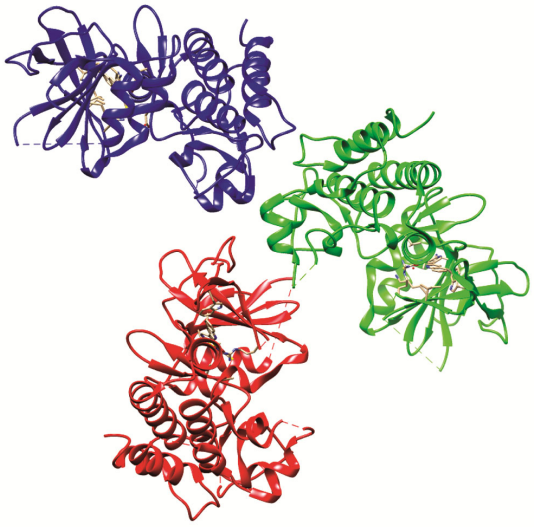

Figure 4 — COT Kinase 3D diagram represented by using Chimera visualization software

Imidazole ligand have many pharmacological properties and play an important role in biochemical processes (Lambardino and Wiseman, 1974). Three dimensional (3D) structures of the compounds were converted from CIF Format to Mol2 format by Marvin Sketch (Csizmadia, 1999).

Vital hydrogen atoms in the protein molecule, Kollman united atom type charges, and solvation parameters were added with the aid of AutoDock tools (Morris et al., 1998). AutoDock Tools used to simulate the binding conformations between the compounds and protein. AutoDock with grid maps of (60×60×60) was applied to explore the binding sites of the target protein. The sites with lowest binding energies were further analyzed using AutoDock.

The entire docking calculations were performed using Autodock docking module program. It performs flexible protein-ligand docking and searches for favorable interactions between one typically small ligand molecule and a typically larger protein molecule. Docking process, wherein protein preparation inhibited refinement is carried out with a maximum of 20 poses, wherein the side chains are optimized and refinement of residues takes place, if the ligand poses are within 5.0Å. The best docked structure was chosen by docking score and the number of amino acids matches (hydrogen bonds) with original drug complex.

The docking energy and hydrogen bonding interactions of the benzoimidazole compound and co-crystallized ligand are given in Table V. X-ray crystal structure of the Cancer Osaka Thyroid Kinase Receptor active site showing the key hydrogen contacts between inhibitor and enzyme is depicted in Figure 5. The co-crystallized ligand in the Cancer Osaka Thyroid Kinase Receptor active site showing the key hydrogen contacts between inhibitor and enzyme is shown in Figure 6. The surface diagram showing the title compound docked at the active site of Cancer Osaka Thyroid Kinase Receptor is depicted in Figure 7.

Table V — Hydrogen bond interactions of Benzodimidazole with amino acids at the active site of Cancer Osaka Thyroid Kinase Receptor

Compd	Docking Score	Hydrogen Bonding Interactions			Hydrophobic
		Donor	Acceptor	Distance (Å)	
Benzodimidazole	−7.1	–	–	–	GLU220 HIS319 PRO154 TYR293 THR290
Co-Crystal	−6.9	ARG146(N-H)	N*	3.4	
		(O-H)	O*	3.5	
		ASP270(O…H)	N*	3.1	
		ASN258(O…H)	N*	3.0	
		(O-H)	N*	3.8	
		SER257(O-H)	N*	3.3	

* Ligand

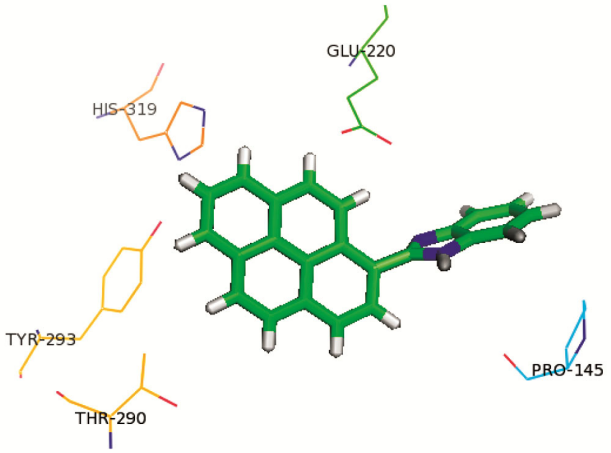

Figure 5 — The title compound in the Cancer Osaka Thyroid Kinase Receptor active site showing key hydrogen contacts between Benzodimidazole inhibitor and enzyme

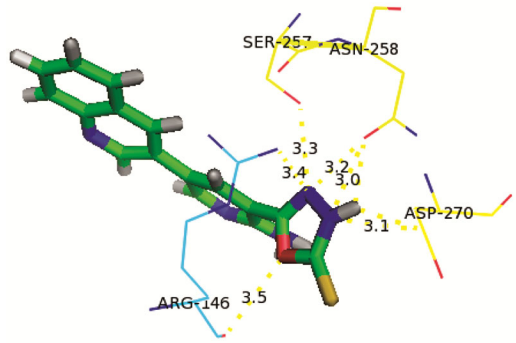

Figure 6 — The co-crystallized ligand in the Cancer Osaka Thyroid Kinase Receptor active site showing the key hydrogen contacts between inhibitor and enzyme

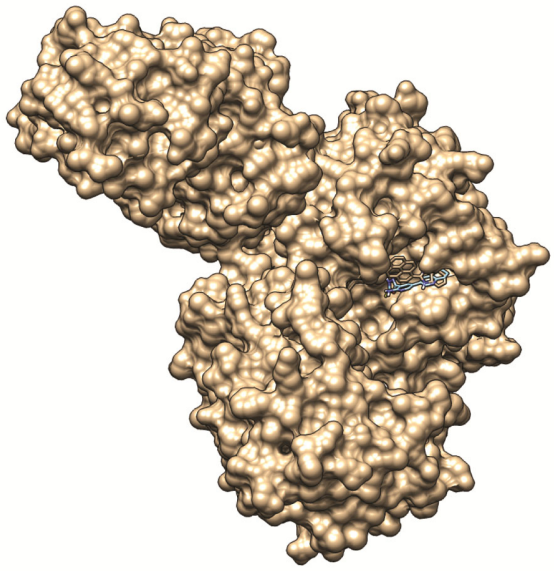

Figure 7 — Surface diagram showing the Benzodimidazole docked at the active site of Ribonucleotide Reductase

Molecular docking analysis of Benzodimidazole indicated that hydrogen bond and hydrophobic are four major interactions (GLU220; HIS319; PRO154; TYR293 and THR290) incorporating the attachment of this ligand to Cancer Osaka Thyroid Kinase acceptor. The co-crystallized ligand also docked well and it shows better interactions with active residues. The results show that the title Benzodimidazole having better binding energy and the co-crystallized ligand have comparable interactions. It is indicated that Benzodimidazole has better ligand protein interactions and reflected that Benzodimidazole will have better antimicrobial character. The expected binding mode and binding orientation and electronic properties enabled optimization to Benzodimidazole as a more potent second-generation lead.

Hirshfeld Surface Analysis

Hirshfeld surface analysis (Spackman & Jayatilaka, 2009) and 2D fingerprint plots (McKinnon et al., 2007) were performed using CrystalExplorer17 (Turner et al., 2017), using standard surface resolution with the three-dimensional surface resolution with the three-dimensional dnorm surfaces plotted over a fixed colour scale of −0.6439 (red) to 1.2824 (blue) a.u.

The 2D fingerprint plots depicts type of intermolecular contacts present in the molecule, and also relative contribution from each type of intermolecular interaction present in the molecule towards the packing of Hirshfeld surface area and it is illustrated in the Figure 8. Further 2D finger plots revealed major contribution to the packing of molecule are (i) H...H-(43.2%), (ii) C…H-(42.4), (iii)

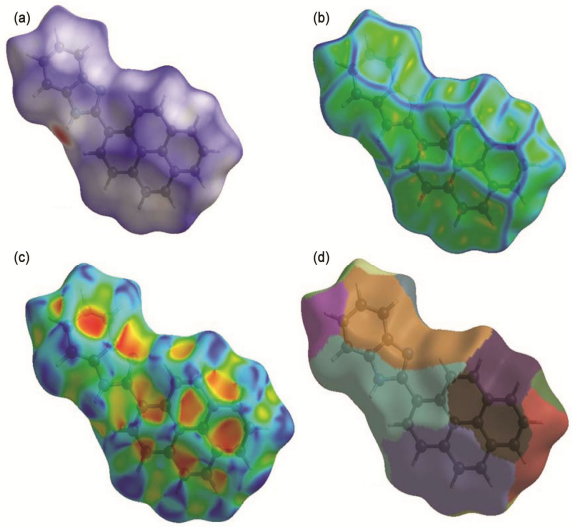

Figure 8 — Hirshfeld surface analysis (a) dnorm, (b) curvedness, (c) shape index and (d) fragment mapped for visualizing the inter contacts of the title compound

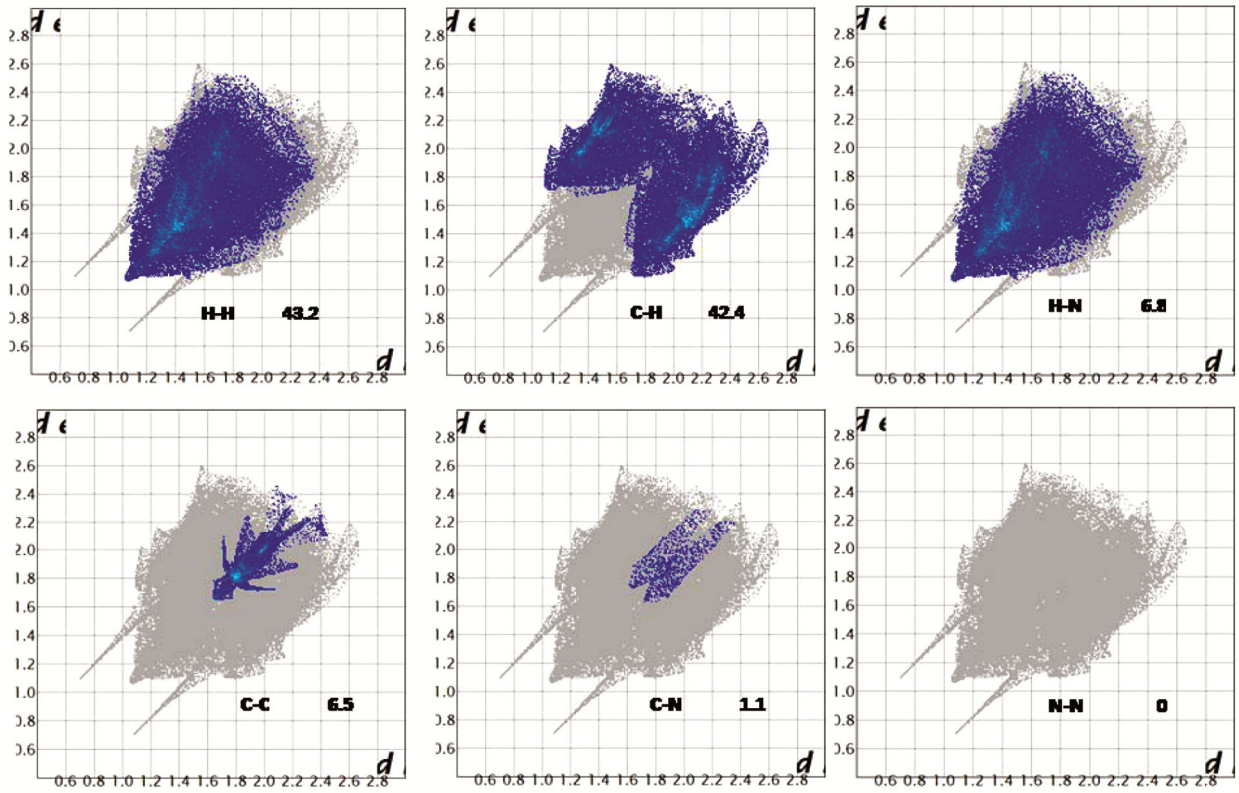

Figure 9 — The outline of the full 2D fingerprint is shown in gray. di is the closest internal distance from a given point on the Hirshfeld surface and de is the closest external contacts

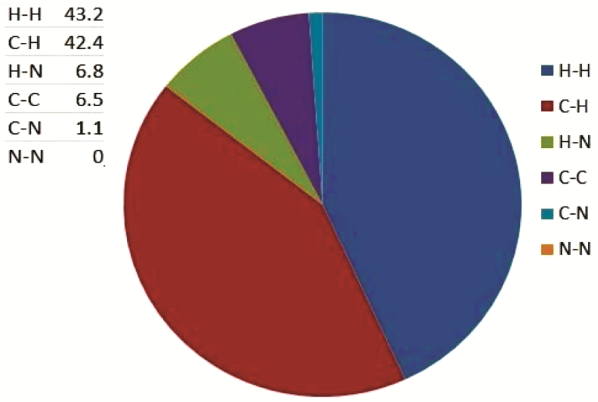

Figure 10 — 2D visualization of percentage of each pair of hydrogen bond contacts

H...N-(6.8%) and (iv) C…C- (6.5%), is shown in the form of spikes, while that of minor contribution (v) C...N-(1.1%), (vi) N...N-(0.0%) also shown in Figure 9 indicates full. Figure 10 percentage of each pair of contact is illustrated in pie chart.

Application

The precise measurement of atomic positions, bond lengths, bond angles in a molecule and also the compound exhibited high binding affinity for anti-cancer activity.

Conclusions

The benzoimidazole compound is crystallized into orthorhombic crystal system with the space group of Pna21. The crystal structure is stabilized with an intra and intermolecular hydrogen bond type of N-H...N interaction. The molecular docking result showed that based on the benzoimidazole compound has good binding affinity with kinase target protein. Further hirshfeld surface analysis and 2D fingerprint plots revealed H...H, H...Cl and H...C are the major contribution in the crystal packing.

Acknowledgements

The authors are grateful to SAIF, IIT Madras for data collection.

References

1 Gharib A, Hashemipour Khorasani B Rh, Jahangir M, Roshani M, Bakhtiari L & Mohadeszadeh S, *Bulg Chem Comm*, 46 (2014) 165.

2 Trujillo I, Kiefer J R, Huang W, Thorarensen A, Xing L, Caspers N L, Day J E, Mathis K J, Kretzmer K K, Reitz B A, Weinberg R A, Stegeman R A, Wrightstone A, Christine L, Compton R & Li X, *Bioorg Lett*, 19 (2009) 908.

3 Chang L L, Sidler K L, Cascieri M A, de Laszlo S, Koch G, Li B, MacCoss M, Mantlo N, O'Keefe S, Pang M,

Rolando A & Hagmann W K, *Bioorg Med Chem Lett*, 11 (2001) 2549.
4 King A J, Patrick D R, Batorsky R S, Ho M L, Do H T, Zhang S Y, Kumar R, Rusnak D W, Takle A K, Wilson D M, Hugger E, Wang L, Karreth F, Lougheed J C, Lee J, Chau D, Stout T J, May E W, Rominger C M, Schaber M D, Luo L, Lakdawala A S, Adams J L, Contractor R G, Smalley K S, Herlyn M, Morrissey M M, Tuveson D A & Huang P S, *Cancer Res*, 66 (2006) 11100.
5 Winter C A, Risely E A & Nuss G W, *Proc Soc Exp Biol, New York*, 111 (1962) 544.
6 Bruker A, SAINT and SADABS, Bruker Analytical X-ray Systems, Inc., Madison, Wisconsin, USA (2008).
7 Sheldrick G M, *Acta Cryst*, A64 (2008) 112.
8 Roskoski R, *Pharmacol Res*, 100 (2015) 1.
9 London C A, *Vet Dermatol*, 24 (2013) 181.
10 Gutmann S, Hinniger A, Fendrich G, Druckes P, Antz S, Mattes H, Mobitz H, Ofner S, Schmiedeberg N, Stojanovic A, Rieffel S, Strauss A, Troxler T, Glatthar R & Sparrer H, *J Biol Chem*, 290 (2015) 15210.
11 Lambardino J G & Wiseman E H, *J Med Chem*, 17 (1974) 1182.
12 Csizmadia P, in 'MarvinSketch and MarvinView: Molecule applets for the World Wide Web', http://www.chemaxon.com/marvin (1999).
13 Bikadi Z & Hazai E J, *Cheminf*, 1 (2009) 15.
14 Morris G M, Goodsell D S, et al., *Journal of Computational Chemistry*, 19(14) (1998) 1639.
15 Csizmadia P, "MarvinSketch and MarvinView: molecule applets for the World Wide Web." Proceedings of ECSOC-3, *The Third International Electronic Conference on Synthetic Organic Chemistry*, September 1-30 (1999).
16 McKinnon, J J, Jayatilaka D & Spackman M A, *Chem Commun*, 3814 (2007).
17 Spackman M A & Jayatilaka D, *Cryst Eng Commun*, 11 (2009) 19.
18 Turner M J, McKinnon, J J, Wolff S K, Grimwood D J, Spackman P R, Jayatilaka D & Spackman M A (2017). CrystalExplorer17. University of Western Australia. http://hirshfeldsurface.net